Journal of Control, Automation and Electrical Systems (2021) 32:1344–1355
https://doi.org/10.1007/s40313-021-00754-5

Modeling and Simulation of The UX-6 Fixed-Wing Unmanned Aerial Vehicle

Tri Kuntoro Priyambodo[1] · **Abdul Majid**[1]

Received: 13 August 2019 / Revised: 7 December 2020 / Accepted: 10 June 2021 / Published online: 29 June 2021

Abstract
The flight model plays an important role in the development of the fixed-wing unmanned aerial vehicle (UAV)'s control system. By using the flight model, aircraft motion characteristics could be identified. Therefore, this modeling method is very important in speeding up parameters tuning of autonomous control systems and also to improve safety. The objective of the present research was to build The UX-6 fixed-wing UAV flight models with two approaches. First, the UX-6 UAV model was built analytically by using Datcom + Pro software. Meanwhile, the second model was built empirically based on flight data system identification. Both approaches were compared and analyzed in longitudinal and lateral flight modes. This work observed eight model's parameters, four in longitudinal modes and four in lateral modes. The parameters comparison demonstrated that five analytical model parameters have similar characteristics with empirical model parameters. Three model parameters had different characteristics, therefore, need to be improved. These parameters comparison results indicate that the model can represent the UX-6 UAV aircraft motion characteristics.

Keywords UAV · Fixed-wing aircraft modeling · Datcom + pro · System Identification · Analytical-empirical comparison

1 Introduction

The UX-6 UAV shown in Fig. 1 is a fixed-wing UAV developed by The Department of Computer Science and Electronics, Universitas Gadjah Mada (Priyambodo et al., 2016a). It was designed as an aerial mapping platform with flying wing configuration. The UX-6 is classified as a small UAV with less than 2 m wingspan. The UX-6 UAV autonomous control system is being developed, using a model-based design approach (Aarenstrup, 2015). This approach needs a mathematical or flight model, as the base for system development. Through the flight model, the aircraft attitude and motion could be learned, as well as the aircraft controller design could be simulated like a linear quadratic regulator (LQR) controller (Dhewa et al., 2017) and proportional integral derivative (PID) controller ((Priyambodo & Dharmawan, 2017; Priyambodo et al., 2016b)).

Each UAV has its characteristics, known as model parameters (Napolitano, 2012). A big UAV or manned aircraft usually uses a wind tunnel test to get the model parameters. This method has the best and accurate result, but there are a lot of challenges to be implemented on small UAVs. First, a limited wind tunnel test facility in Indonesia, none of them located in our university. Second, the cost for the wind tunnel test relatively high (especially for build a precision 3D model scale). Third, wind tunnel tests need an experienced operator and data interpreter. From these considerations, the wind tunnel test is incompatible with this research.

This research focuses on how to build a flight model of small fixed-wing UAV like UX-6 UAV using analytical modeling. Analytical modeling was developed based on aircraft geometry data. Then, aircraft geometry data processed using Datcom + Pro software (Galbraith, 2015). Datcom + Pro were widely used to build large fixed-wing UAVs and manned aircraft models at the preliminary design review stage. The analytical model is then validated by comparing with the empirical model. The empirical model was built using the system identification method (Majid et al., 2015). After validation, in the last stage, the analytical model was visualized on the Flight Gear flight simulator. The overall design of this research is shown in Fig. 2.

✉ Tri Kuntoro Priyambodo
mastri@ugm.ac.id

[1] Department of Computer Science and Electronics, Faculty of Mathematics and Natural Science, Universitas Gadjah Mada, Yogyakarta 55281, Indonesia

Fig. 1 UX-6 fixed-wing UAV

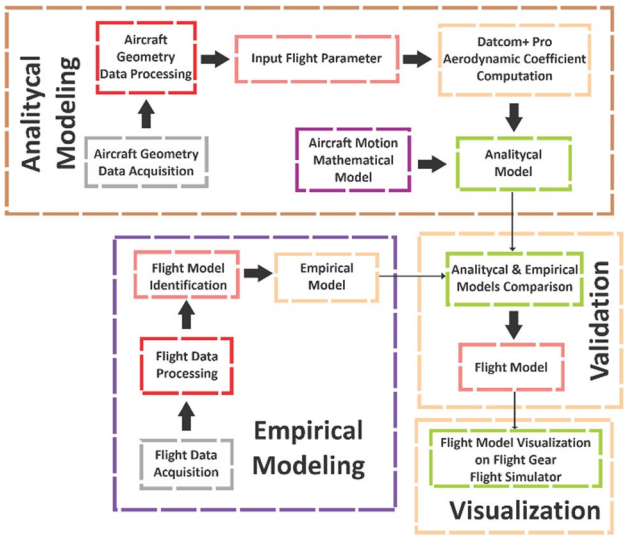

Fig. 2 The overall design of UX-6 fixed-wing UAV modeling

2 The Material and Method

2.1 Flying Wing UAV

Flying wing UAV has some differences if compared with the conventional fixed-wing UAV. On the other hand, conventional fixed-wing UAVs are divided into the fuselage, wings, horizontal stabilizer, and vertical stabilizer, flying wing just has wings. The fuselage and wings were blended. There are no vertical stabilizer and horizontal stabilizer on the flying wing. Flying wing control surface is called elevons (elevators and ailerons). Elevators are for up-down movements and ailerons are for right-left turn movements. The design of the flying wing UAV is shown in Fig. 3.

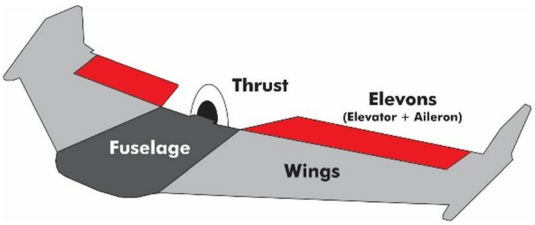

Fig. 3 Design of flying wing UAV

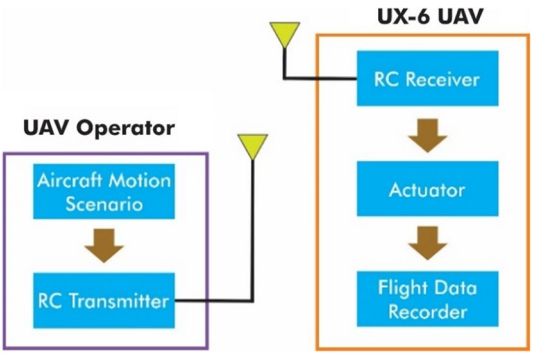

Fig. 4 The hardware diagram

2.2 Hardware

The hardware used in this research consists of the UX-6 aircraft and electronic devices as shown in Fig. 4.

The UX-6 UAV was manually controlled by an operator on the ground for flight data acquisition. There is an onboard flight data recorder for recording an operator input for actuators and an output from the aircraft. An aircraft output was obtained from sensors inside a flight data recorder. A flight data recorder runs the data recording at 5 Hz, while the maximum aircraft movement is at 2 Hz (Tischler, 2006). All aircraft electronic devices connection is shown in Fig. 5.

Figure 6 shows all electronic devices consisting of actuators, flight data recorder, radio controller receiver, and batteries that are implemented onboard the aircraft.

The complete aircraft hardware and specification are shown in Table 1.

2.3 Data Acquisition

UX-6 UAV does not yet have complete data, hence there is a need for data acquisition, both geometry data and flight data.

(1) *Aircraft Geometry Data Acquisition* Aircraft geometry data are required for Datcom + Pro software input, which is then used to build the analytical model. The required aircraft data are as follows:

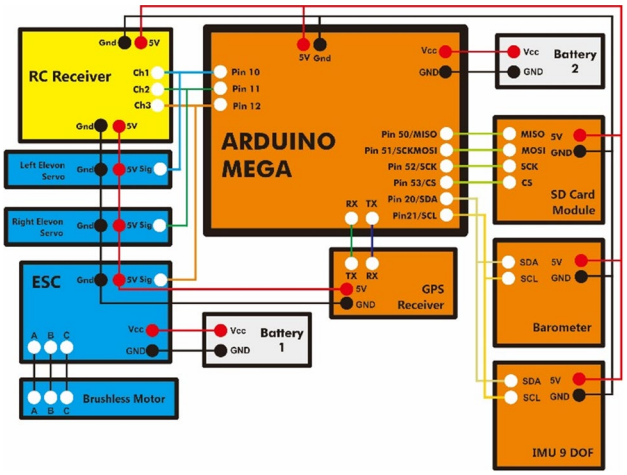

Fig. 5 UX-6 aircraft electronics devices diagram: flight data recorder (orange), actuators (blue), radio control receiver (yellow), and power source (gray) (Color figure online)

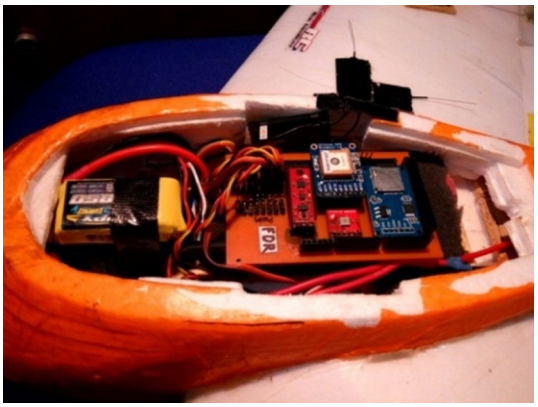

Fig. 6 UX-6 UAV electronic devices

- Aircraft sketch and dimension data.
- Aircraft control surface position.
- Aircraft airfoil data.
- Aircraft moment of inertia data.
- Aircraft weight and center-of-gravity data.

(2) *Flight Data Acquisition* Flight data acquisition include two things, input data and aircraft output. The input data include the signal given by the operator to the actuator (elevator and aileron) through the radio controller, while the output data include the attitude, position, and speed of the aircraft. Flight data acquisition needs to be well planned, to match what is expected. For this research, the input on the plane is a doublet input. Doublet input is a variation in input where a high pulse-width-modulation (PWM) signal was given during the time t and then directly assigned a low PWM signal during time t as well. Doublet inputs are widely used by researchers worldwide in modeling and identification of aircraft models, including the Boeing aircraft manufacturer when identifying the F-15 Eagle fighter aircraft (Smith & Moes, 2003). Figure 7 shows the shape of the input doublet signal.

In this research, modeling will be divided into two modes, longitudinal mode and lateral mode. In longitudinal mode, the doublet input was given on the elevator, then in lateral mode, the doublet input was given on the aileron. Before the doublet input was given, the aircraft is conditioned in trim and level conditions (the aircraft is considered in a state of straight flight and the right-left wing of the aircraft is in the same state horizontally). The diagram of the flight data acquisition procedure is shown in Fig. 8.

The recorded flight data were then processed and converted to a variable that was used for empirical modeling or system identification as shown in Fig. 9.

2.4 Analytical Modeling

In the fixed-wing UAV flight, there are many forces, velocities, moments, and orientations that work. All could be summarized and visualized in Fig. 10.

In a flight, the aircraft is not always horizontally straight when flying straight ahead (on the X-axis, see Fig. 11) but has an angle-of-attack angle commonly written α (alpha). The aircraft angle-of-attack is the deflection angle of the aircraft on the x-axis caused by the airplane's wing geometry. Similar to angle-of-attack, there is also a sideslip angle (Fig. 11), which is usually written β (beta). The difference is that the sideslip angle is the deflection on the y-axis due to the air/wind from the side that concerns the vertical stabilizer of the aircraft. Equations 1 and 2 are for finding α and β.

$$\alpha = \tan^{-1}\frac{w}{u} \tag{1}$$

$$\beta = \tan^{-1}\left(\frac{v}{\sqrt{u^2 + w^2}}\right) \tag{2}$$

The Euler angle was used for the aircraft orientation as shown in Fig. 11, which has the following reference:

a. Z-axis leads downward (same as the direction of the gravity vector). The angle rotation on this axis is called yaw (ψ).
b. X-axis leads forward. The angle rotation on this axis is called roll (φ).
c. Y-axis leads rightward. The angle rotation on this axis is called pitch (θ).

Table 1 Aircraft hardware and specification

Hardware		Specification
Aircraft	UX-6 Fixed-wing UAV	Flying wing
		Polyfoam material
Actuator	*Electric motor*	Brushless 800 kV
		12 inch propeller
		11.1 V
		950 gr Thrust
	Mini servo	5–6 V
		Torque 1.6 kg
		9 gr Weight
Flight data recorder	Arduino Mega 2560	ATMega 2560 Microcontroller
		5 V
		16 MHz speed & 256 Kb flash memory
		54 Digital & 16 Analog I/O
	Sensors:	ADXL345 Accelerometer
	9 DoF sensor stick IMU	ITG3200 Gyroscope
		HMC5883L Magnetometer
	Barometer	BMP085 Barometer
	GPS receiver	MTK3339 GPS
	Data recorder:	*Micro* SD *card*
		3.3 V Voltage operation
		SPI communication
Radio controller	9 Channel transmitter	PPM receiver output
	8 Channel receiver	2.4 GHz frequency
Power source	Lithium polymer battery	3 cell 11.1 V 2200mAH 30C
		2 cell 7.4 V 850mAH 20C

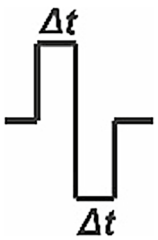

Fig. 7 Doublet input

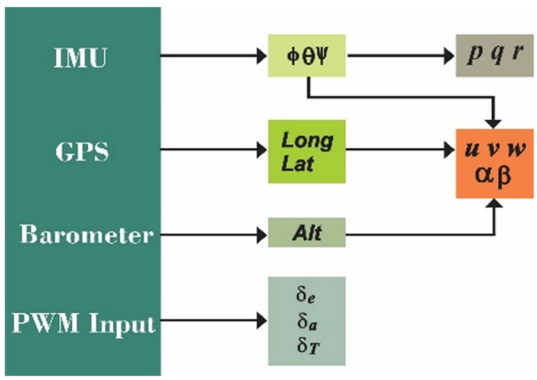

Fig. 9 The recorded flight data processing

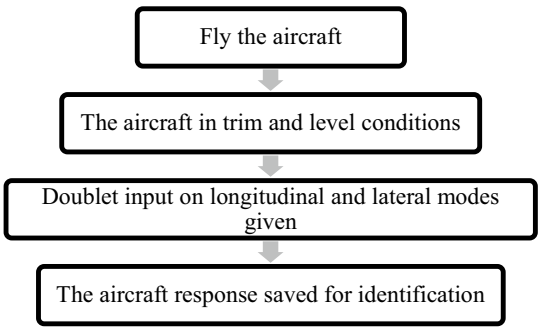

Fig. 8 UX-6 UAV flight data acquisition procedures

In an aircraft motion modeling, one of the parameters used is the angular velocity on the x, y, and z axes. The angular velocity is called the variables p, q, and r. To find it is used Eq. 3.

$$\begin{bmatrix} p \\ q \\ r \end{bmatrix} = \begin{bmatrix} 1 & 0 & -\sin\theta \\ 0 & \cos\phi & \cos\theta\sin\phi \\ 0 & -\sin\phi & \cos\theta\cos\phi \end{bmatrix} \begin{bmatrix} \phi' \\ \theta' \\ \psi' \end{bmatrix} \tag{3}$$

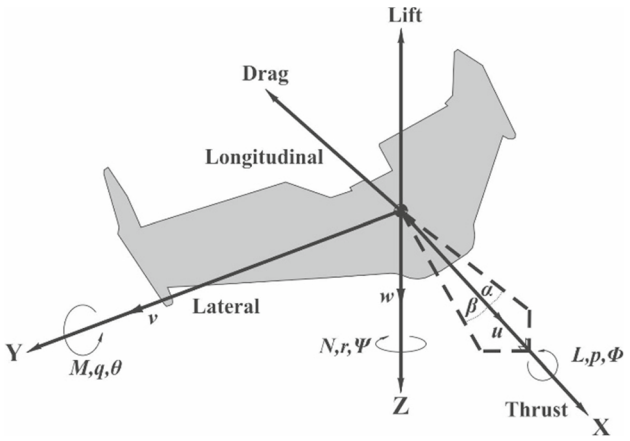

Fig. 10 Aircraft forces, velocities, moments, and orientations definitions

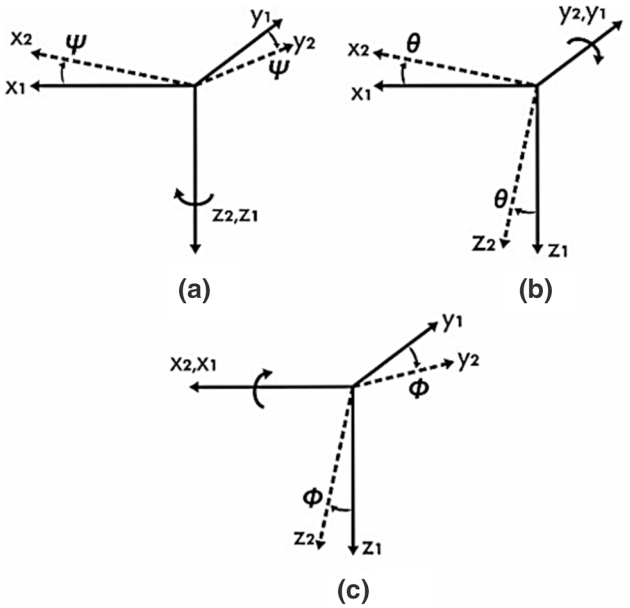

Fig. 11 Euler angle Φ, θ, and ψ to determine the orientation of a flying plane. **a** Yaw rotation on the Z-axis **b** Pitch rotation on Y-axis. **c** Roll rotation on X-axis

where

$$\phi',\ \theta', \psi' \ = \frac{\mathrm{d}\phi}{\mathrm{d}t}, \frac{\mathrm{d}\theta}{\mathrm{d}t}, \frac{\mathrm{d}\psi}{\mathrm{d}t}$$

In addition to the angular velocity, the translation velocities are required for each of the x, y, and z axes. The translational velocities of each axis are called the variables u, v, and w. The variables u, v, and w are determined by data changes in variable longitude, latitude, and altitude. Then, it is combined with the orientation of the Euler angle, thus producing u', v', and w' derived from Eq. 4.

$$\begin{bmatrix} \frac{\mathrm{dx}}{\mathrm{d}t} \\ \frac{\mathrm{dy}}{\mathrm{d}t} \\ \frac{\mathrm{dz}}{\mathrm{d}t} \end{bmatrix} = \begin{bmatrix} C\theta C\psi & S\phi S\theta C\psi - C\phi S\psi & C\phi S\theta C\psi + S\phi S\psi \\ C\theta S\psi & S\phi S\theta S\psi + C\phi C\psi & C\phi S\theta S\psi - S\phi C\psi \\ -S\theta & S\phi C\theta & C\phi C\theta \end{bmatrix} \begin{bmatrix} u \\ v \\ w \end{bmatrix}$$

where

$$S\phi,\ S\theta,\ S\psi = \sin\phi,\ \ \sin\theta, \sin\psi$$

$$C\phi, C\theta,\ C\psi = \cos\phi, \cos\theta,\ \ \cos\psi$$

The flight dynamics that work on fixed-wing can be divided into two modes, namely the longitudinal and lateral modes (Nelson, 1998). Longitudinal modes include translational motion on the X and Z axes and rotational motion around the Y-axis. The rotary motion around the Y-axis will change the pitch angle. The motion in the longitudinal mode plays a role in the up and down movement of the aircraft. In the dynamics of aircraft flying, the longitudinal mode is influenced by the thrust and elevator. The longitudinal mode is determined by Eqs. 5 to 8

– Forces equations

$$u' + qw - rv = X/m - g\ \sin\theta \tag{5}$$

$$w' + pv - qu = Z/m + g\ \cos\theta\ \cos\phi \tag{6}$$

– Moments equations

$$M = I_y q' + rp\left(I_x - I_y\right) + I_{xz}\left(p^2 - r^2\right) \tag{7}$$

– Pitch orientation

$$\theta' = q\ \cos\phi - r\ \sin\phi \tag{8}$$

The lateral mode includes translational motion on the Y-axis and rotational motion on the X and Z axes. The lateral mode is affected by the aileron. Lateral or sometimes called directional mode is used for aircraft's turn movement. The lateral mode is determined by Eqs. 9 to 12

– Forces equation

$$v' + ru - pw = Y/m + g\ \cos\theta_0\ \sin\phi \tag{9}$$

– Moments equations

$$L = I_x p' - I_{xz} r' + qr\left(I_z - I_y\right) - I_{xz} pq \tag{10}$$

$$N = -I_{xz} p' + I_z r' + pq\left(I_y - I_x\right) + I_{xz} qr \tag{11}$$

– Roll orientation

$$\phi' = p + (q\ \sin\phi - r\ \cos\phi)\ \tan\theta \tag{12}$$

All of the equations that work both longitudinal and lateral modes are necessary to elaborate and add flight assumptions (linear model and ignore flight disturbances like wind, thermal, and weather). Then, we find the general equations of the longitudinal mode flight model in the form of the state-space model structure shown in Eq. 13.

$$\begin{bmatrix} \Delta\dot{u} \\ \Delta\dot{\alpha} \\ \Delta\dot{q} \\ \Delta\dot{\theta} \end{bmatrix} = \begin{bmatrix} X_u & X_w & X_q + w_0 & -g\cos\theta_0 \\ \frac{Z_u}{u_0} & \frac{Z_w}{u_0} & Z_q - w_0 & \frac{-g\sin\theta_0}{u_0} \\ M_u & M_w & M_q & 0 \\ 0 & 0 & \cos\phi_0 & 0 \end{bmatrix} \begin{bmatrix} \Delta u \\ \Delta\alpha \\ \Delta q \\ \Delta\theta \end{bmatrix} + \begin{bmatrix} X_{\delta_e} & X_{\delta_T} \\ Z_{\delta_e} & 0 \\ M_{\delta_e} & 0 \\ 0 & 0 \end{bmatrix} \begin{bmatrix} \Delta\delta_e \\ \Delta\delta_T \end{bmatrix} \tag{13}$$

Then, for lateral mode is the same as the longitudinal mode. Equation 14 is obtained as a representation of the general equation of the lateral mode flight model.

$$\begin{bmatrix} \Delta\dot{\beta} \\ \Delta\dot{p} \\ \Delta\dot{r} \\ \Delta\dot{\phi} \end{bmatrix} = \begin{bmatrix} \frac{Y_u}{u_0} & \frac{Y_p + w_0}{u_0} & \frac{-(u_0 - Y_r)}{u_0} & \frac{g\cos\theta_0}{u_0} \\ L_v & L_p & L_r & 0 \\ N_v & N_p & N_r & 0 \\ 0 & 1 & \tan\theta_0 & 0 \end{bmatrix} \begin{bmatrix} \Delta\beta \\ \Delta p \\ \Delta r \\ \Delta\phi \end{bmatrix} + \begin{bmatrix} 0 \\ L_{\delta_a} \\ N_{\delta_a} \\ 0 \end{bmatrix} [\Delta\delta_a] \tag{14}$$

The general linear equations of the longitudinal and lateral modes were obtained, the next is to calculate to fill each variable with values corresponding to the characteristics of the aircraft modeled using the Datcom + Pro software.

The Datcom + Pro output is divided into static and dynamic aerodynamic coefficients that are used for derivative stability calculation. The calculations also required the aircraft data shown in Table 2.

The derivative stability calculations are divided into longitudinal mode and lateral mode (Stevens & dan Lewis, 2003). Table 3 shows the formula for longitudinal mode derivative stability calculations (Bagheri, 2014).

The lateral mode derivative stability calculations are shown in Table 4 (Bagheri, 2014).

In the last analytical modeling stage, the derivative stability calculation results are then arranged using the general linear equations, Eq. 13 for longitudinal mode and Eq. 14 for lateral modes.

2.5 Empirical Modeling

Analytical models need to be compared with another model for analysis purposes. The empirical models have been built based on flight data. Empirical models use system identification techniques. System identification techniques have required input and output data when flying for system identification. The data used for system identification are selected on a particular part only, i.e., when the aircraft control surface is given a doublet input. This empirical model uses a state-space model structure. Slightly different from the analytical model, the common

Table 2 Aircraft data for derivative stability calculation

Notation	Definition
m	Aircraft weight
S	Wing area
C_bar	Mean aerodynamic chord
b	Wingspan
g	Earth gravity acceleration
Rho	Air density
Alpha	Angle-of-attack
Q	Dynamic air pressure
theta0	Pitch angle on trim condition
u0	Translation velocity in *x*-axis
Ix	*x*-axis moment inertia
Iy	*y*-axis moment inertia
Iz	*z*-axis moment inertia
Va	Air velocity in trim condition
S_prop	Propeller sweep area
C_prop	Propeller coefficient
K	Propeller constanta

Table 3 Longitudinal mode derivative stability calculation

Derivative	Formula
X_u	$\frac{u\rho S}{m}\left[C_{X_0} + C_{X_\alpha}\alpha + C_{X_{\delta_e}}\delta_e\right] - \frac{\rho SwC_{x_\alpha}}{2m} - \frac{\rho S_{prop}C_{prop}u}{m}$
X_w	$\frac{w\rho S}{m}\left[C_{X_0} + C_{X_\alpha}\alpha + C_{X_{\delta_e}}\delta_e\right] - \frac{\rho SuC_{x_\alpha}}{2m} - \frac{\rho S_{prop}C_{prop}u}{m}$
X_q	$-w + \frac{\rho V_a SC_{x_q}c}{2m}$
X_{δ_e}	$\frac{\rho V_a^2 SC_{x_{\delta_e}}}{2m}$
X_{δ_T}	$\frac{\rho S_{prop}C_{prop}K\delta_T}{m}$
Z_u	$\frac{u\rho S}{m}\left[C_{Z_0} + C_{Z_\alpha}\alpha + C_{X_{\delta_e}}\delta_e\right] - \frac{\rho SwC_{Z_\alpha}}{2m}$
Z_w	$\frac{w\rho S}{m}\left[C_{Z_0} + C_{Z_\alpha}\alpha + C_{X_{\delta_e}}\delta_e\right] - \frac{\rho SuC_{Z_\alpha}}{2m}$
Z_q	$u + \frac{\rho V_a SC_{Z_q}c}{2m}$
Z_{δ_e}	$\frac{\rho V_a^2 SC_{Z_{\delta_e}}}{2m}$
M_u	$\frac{u\rho Sc\left[C_{M_0} + C_{M_\alpha}\alpha + C_{M_{\delta_e}}\delta_e\right]}{I_y} - \frac{\rho ScC_{M_\alpha}w}{2I_y}$
M_w	$\frac{w\rho Sc\left[C_{M_0} + C_{M_\alpha}\alpha + C_{M_{\delta_e}}\delta_e\right]}{I_y} - \frac{\rho ScC_{M_\alpha}u}{2I_y}$
M_q	$\frac{\rho V_a Sc^2 C_{M_q}}{2I_y}$
M_{δ_e}	$\frac{\rho V_a^2 SC_{M_{\delta_e}}}{2I_y}$

Table 4 Lateral mode derivative stability calculation

Derivative	Formula
Y_β	$\frac{QS}{m}C_{Y_b}$
Y_p	$\frac{QSb}{2u_0 m}C_{Y_p}$
Y_r	$\frac{QSb}{2u_0 m}C_{Y_r}$
Y_{δ_a}	$\frac{QS}{m}C_{Y_{\delta_a}}$
N_β	$\frac{QS_b}{2I_z}C_{N_b}$
N_p	$\frac{QSb^2}{2u_0 I_x}C_{N_p}$
N_r	$\frac{QSb^2}{2u_0 I_x}C_{N_r}$
N_{δ_a}	$\frac{QS_b}{I_z}C_{\delta_a}$
L_β	$\frac{QS_b}{2I_x}C_{l_b}$
L_p	$\frac{QSb^2}{2u_0 I_x}C_{l_p}$
L_r	$\frac{QSb^2}{2u_0 I_x}C_{l_r}$
L_{δ_a}	$\frac{QS_b}{I_x}C_{l_{\delta_a}}$
$Q = \frac{1}{2}\rho V_a^2$	

state-space model structure was used, not a motion equation constructed from the description of force, moment, and orientation acting on the plane. This type of identification system is known as black-box system identification (Triputra et al., 2016). Identify the system using the system identification toolbox, one of the tools in the MATLAB software.

2.6 Visualization

A model can be displayed or presented in various ways. The most common way is with mathematical equations and drawing graphs. To further simplify the attitude of unmanned UX-6 fixed-wing aircraft, this model has been visualized and simulated in flight simulators. Visualization used two software, Simulink and Flight Gear flight simulator. The program is designed using Simulink, in which flight dynamics consisting of moments and forces acting on the plane, aircraft flight equations, models of actuators, and aerodynamic coefficients derived from the modeling done. Visualization of flight using flight will show the model of the plane and the parameters of the aircraft, i.e., attitude (angle of a roll, pitch, and yaw) and the position of the aircraft (altitude, longitude, latitude). The simulator program built can be seen in Fig. 12. The program was developed based on the Beaver DHC-2 simulator program (Mathwork, 2015).

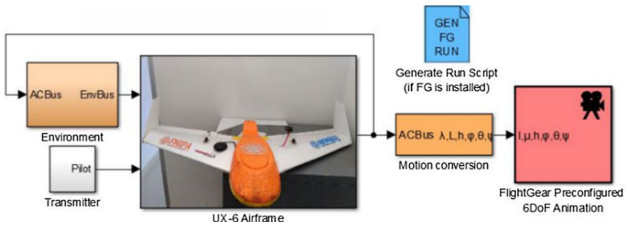

Fig. 12 UX-6 UAV visualization block diagram

3 Results and Discussion

3.1 Data Acquisition

(1) Aircraft Geometry Data Acquisition: Aircraft geometry data acquisition results are shown in Table 5.
(2) *Flight Data Acquisition:* Flight data acquisition is performed in the morning to get the best weather (clear and the wind speed relative is zero). We did two flights, one for the main data and the other as backup data. The UX-6 flight path that is used as the main data is shown in Fig. 13.

3.2 Analytical Model

The Datcom + Pro software is used for calculation needs aircraft geometry data and flight condition scenario. Aircraft geometry data are based on UX-6 UAV geometry data. There is a slight difference compared with the real aircraft. Datcom + Pro could not generate wings winglet geometry, so winglet was not considered in this

Table 5 UX-6 UAV geometry data

Parameters	Value
Aircraft length (cm)	47
Fuselage width (cm)	17.5
Fuselage height (cm)	8
Weight (kg)	0.944
Moment inertia (kg.m^2)	$I_x = 0.0273$ $I_y = 0.0016$ $I_z = 0.0497$
CG from nose (cm)	25
Chord tip(cm)	17
Chord root (cm)	29
Taper ratio	0.57
Mean aerodynamic chord (cm)	23.9
Semi-span theoritical panel (cm)	50.1
Semi-span exposed panel (cm)	41.6
Sweep wing angle (°)	30

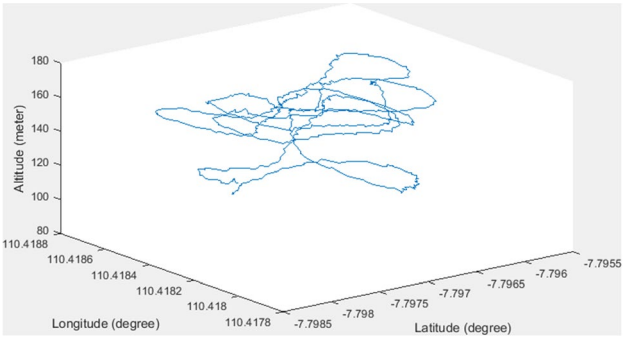

Fig. 13 UX-6 flight path

```
$FLTCON NMACH=1.0, MACH(1)=0.044, NALPHA=8.0,
ALSCHD(1)=-4.0,-2.0,0.0,2.0,4.0,6.0,8.0,10.0,
NALT=1.0, ALT(1)=67.0, WT=9.257, LOOP=1.0$

$OPTINS SREF=1692.16, CBARR=23.89, BLREF=100.2$
$SYNTHS   XCG=25.0,   ZCG=0.0,   XW=8.0,   ZW=0.6,
ALIW=0.0$
$BODY NX=19.0,
X(1)=0.0,0.2,0.5,1.0,4.0,5.0,5.9,7.0,8.0,9.0,11.
0,12.0,13.5,15.0,35.5,35.5,43.6,47.0,47.,
R(1)=0.0,1.2,2.5,3.6,6.5,7.1,7.5,7.9,8.1,8.3,8.5
,8.6,8.75,8.0,5.5,5.5,3.0,2.5,2.5,
ZU(1)=1.5,1.9,2.8,3.5,5.8,7.2,7.3,7.4,7.5,7.6,7.
7,7.8,7.9,8.0,5.5,3.5,7.0,7.0,3.5,
ZL(1)=1.5,1.0,0.7,0.4,0.0,0.0,0.0,0.0,0.0,0.0,0.
0,0.0,0.0,0.0,0.0,0.0,0.0,0.0,3.5$

$WGPLNF   CHRDTP=17.0,   SSPNE=41.6,   SSPN=50.1,
CHRDR=29.7, CHSTAT=0.0, SAVSI=30.0, TWISTA=-1.0,
DHDADI=0.0, TYPE=1.0$

$WGSCHR TYPEIN=1.0, NPTS=16.0, DWASH=1.0,
XCORD=0.000000,0.008824,0.023529,0.070588,0.1675
47,0.252941,0.341176,0.420588,0.532353,0.611765,
0.626471,0.741176,0.758824,0.814706,1.0,1.0,
YUPPER=0.002941,0.011765,0.017647,0.029412,0.058
824,0.082353,0.091176,0.082353,0.058824,0.047059
,0.047059,
0.029412,0.023529,0.020588,0.011765,0.011765,
YLOWER=0.002941,-0.011765,-0.020588,-0.029412,-
0.035294,-0.035294,-0.035294,-0.035294,-
0.035294,-0.035294,-0.029412,-0.026471,-
0.026471,-0.017647,-0.008824, 0.011765$
```

Fig. 14 Datcom + Pro input for UX-6 UAV geometry and flight scenario

calculation. A flight condition was equated with the UX-6 UAV steady-state flight condition (obtained from flight data). The UX-6 UAV steady-state flight condition was predicted to occur at AoA of 4 degrees, velocity of 15.3 m/s, and an altitude of 67 m. Figure 14 shows UX-6 UAV geometry and flight scenario data were input to Datcom + Pro software.

The UX-6 UAV geometry data and flight scenario that entered to Datcom + Pro software generated the aircraft 3D model and the aircraft calculated aerodynamic coefficients. The UX-6 UAV 3D model is shown in Fig. 15.

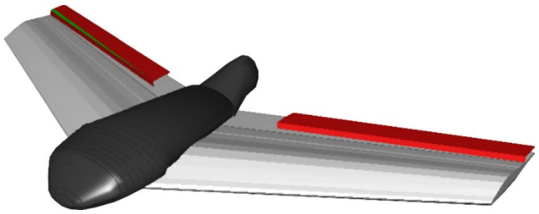

Fig. 15 UX-6 3D model

Table 6 UX-6 UAV static aerodynamic coefficients

Coefficient	Value
Longitudinal mode	
C_{L_0}	−0.53
C_{D_0}	0.049
C_{M_0}	0.1281
C_{X_0}	−0.0848
C_{Z_0}	0.5255
C_{L_α}	*6.097*
C_{D_α}	0.028
C_{M_α}	−0.6046
C_{X_α}	0.3857
C_{Z_α}	−6.0849
C_{L_q}	5.0637
C_{D_q}	0
C_{M_q}	−1.37
C_{X_q}	0.3436
C_{Z_q}	−5.0520
Lateral mode	
C_{Y_r}	0
C_{l_r}	−0.0191
C_{n_r}	*−0.0067*
C_{Y_β}	*−0.2747*
C_{l_β}	0.0043
C_{n_β}	−0.0007
C_{Y_p}	*−0.0059*
C_{l_p}	−0.4815
C_{n_p}	−0.0015

The calculated aerodynamic coefficients of Datcom + Pro were divided into static and dynamic aerodynamic coefficients. The static aerodynamic coefficients were derived from the calculation of the plane's geometry shape. The

Table 7 UX-6 UAV dynamic aerodynamic coefficients

Longitudinal mode		Lateral mode	
Coefficient	Value	Coefficient	Value
$C_{L_{\delta_e}}$	0.386	$C_{Y_{\delta_a}}$	0
$C_{D_{\delta_e}}$	0.0077	$C_{l_{\delta_a}}$	−0.0751
$C_{M_{\delta_e}}$	−0.2203	$C_{n_{\delta_a}}$	−0.0009

results from the static aerodynamic coefficients calculation are shown in Table 6.

The dynamic aerodynamic coefficient is obtained from the movement or deflection of the plane's control surface (elevator and aileron). The results from the static aerodynamic coefficients calculation are shown in Table 7.

The obtained static and dynamic aerodynamic coefficients then become the base for the stability derivative calculation. The resulting stability derivative is organized into Eqs. 13 and 14. The analytical model of the UX-6 UAV is shown on Eq. 15 for longitudinal mode.

$$\begin{bmatrix} \Delta\dot{u} \\ \Delta\dot{\alpha} \\ \Delta\dot{q} \\ \Delta\dot{\theta} \end{bmatrix} = \begin{bmatrix} -5.7149 & 0.4779 & 0.1333 & -9.7874 \\ 0.2940 & -9.7749 & 12.8036 & -0.6656 \\ 17.8584 & -136.5561 & -74.9010 & 0 \\ 0 & 0 & 1.0 & 0 \end{bmatrix} \begin{bmatrix} \Delta u \\ \Delta\alpha \\ \Delta q \\ \Delta\theta \end{bmatrix} + \begin{bmatrix} 0.4597 & 4.7302 \\ -9.5796 & 0 \\ -771.3592 & 0 \\ 0 & 0 \end{bmatrix} \begin{bmatrix} \Delta\delta_e \\ \Delta\delta_T \end{bmatrix}$$

The lateral mode of UX-6 UAV analytical model is shown in Eq. 16.

$$\begin{bmatrix} \Delta\dot{\beta} \\ \Delta\dot{p} \\ \Delta\dot{r} \\ \Delta\dot{\phi} \end{bmatrix} = \begin{bmatrix} -0.4859 & -0.0053 & -14.6000 & 9.5040 \\ 0.2682 & -15.3192 & -0.6077 & 0 \\ -0.0240 & -0.0262 & -0.1171 & 0 \\ 0 & 1 & 0.068 & 0 \end{bmatrix} \begin{bmatrix} \Delta\beta \\ \Delta p \\ \Delta r \\ \Delta\phi \end{bmatrix} + \begin{bmatrix} 0 \\ -68.4010 \\ -0.4503 \\ 0 \end{bmatrix} \begin{bmatrix} \Delta\delta_a \end{bmatrix} \tag{16}$$

The analytical model results are then compared with the empirical model for model analysis.

3.3 Empirical Model

After the flight data are obtained, the next is to determine trim conditions. The trim condition is when $u \neq 0$, $w = 0$, $q = 0$, and $\theta \neq 0$. The UX-6 UAV trim conditions are given in the following Table 8.

Using the MATLAB's system identification toolbox (SITB) software, a model that represents UX-6 UAV was built. Similar to the analytical model, the empirical model is divided into longitudinal and lateral modes. Equation 17 shows the empirical model for UX-6 UAV longitudinal mode.

$$\begin{bmatrix} \Delta\dot{u} \\ \Delta\dot{\alpha} \\ \Delta\dot{q} \\ \Delta\dot{\theta} \end{bmatrix} = \begin{bmatrix} -7.885 & -6.109 & -3.328 & -4.334 \\ 3.406 & 1.742 & 5.731 & 2.15 \\ -0.9673 & -1.311 & 0.7918 & 2.72 \\ 2.856 & 2.527 & -0.7077 & 1.28 \end{bmatrix} \begin{bmatrix} \Delta u \\ \Delta\alpha \\ \Delta q \\ \Delta\theta \end{bmatrix} + \begin{bmatrix} -5.222 & -39.47 \\ -1.155 & -16.03 \\ -2.321 & 10.53 \\ 2.552 & 28.68 \end{bmatrix} \begin{bmatrix} \Delta\delta_e \\ \Delta\delta_T \end{bmatrix} \tag{17}$$

Equation 18 shows the empirical model for UX-6 UAV lateral mode.

$$\begin{bmatrix} \Delta\dot{\beta} \\ \Delta\dot{p} \\ \Delta\dot{r} \\ \Delta\dot{\phi} \end{bmatrix} = \begin{bmatrix} -0.06034 & -1.324 & 1.423 & -0.1505 \\ 3.96 & -1.866 & 2.701 & 4.011 \\ -2.08 & -1.389 & -0.7703 & -0.4127 \\ 0.2957 & 1.35 & -1.02 & -0.4969 \end{bmatrix} \begin{bmatrix} \Delta\beta \\ \Delta p \\ \Delta r \\ \Delta\phi \end{bmatrix} + \begin{bmatrix} [-1.923 \\ 0.6245 \\ -0.9213 \\ -1.379 \end{bmatrix} \begin{bmatrix} \Delta\delta_a \end{bmatrix} \tag{18}$$

The empirical model results were validated by simulation. In a simulation, the empirical model is compared with the real flight data. The empirical model input is the aircraft input data and then the model output was compared with aircraft output data. From the empirical model validation results, the model accuracy is quite good, 73.95% average for longitudinal mode and 75.83% average for lateral mode. Figure 16 shows empirical model validation results for longitudinal mode and Fig. 17 for lateral mode.

3.4 Analytical-Empirical Comparison

The analytical models that have been built are compared with the empirical model for validation. Elevator in longitudinal mode and aileron in lateral mode both were given doublet input shown in Fig. 18.

Comparative results of UX-6 UAV between the analytical model and empirical model are shown in Fig. 19 for longitudinal mode.

The longitudinal mode comparative results showed that three parameters in longitudinal mode [u, theta (θ), and alpha (α)] are quite identical and one parameter (q) is not identical or different waveforms. Figure 20 shows comparative results for lateral mode, two parameters [p and roll (Φ)] are quite identical and two parameters [beta (β) and r] have different waveforms. The identical is when the parameters of the analytical and the empirical model have the same

Table 8 UX-6 UAV trim condition

Parameter	Value (radian)
Pitch angle (θ)	0.0679
Roll angle (ϕ)	−0.0351
Elevator deflection (δ_e)	0.2503
Aileron deflection(δ_a)	0.059

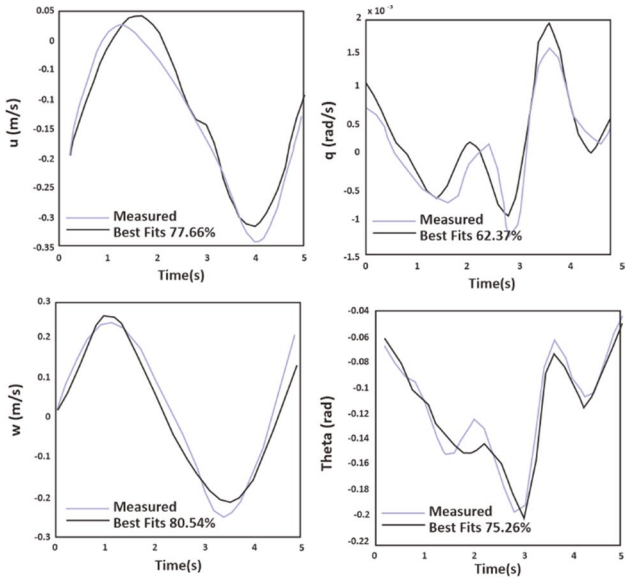

Fig. 16 Empirical model (longitudinal mode) validation results

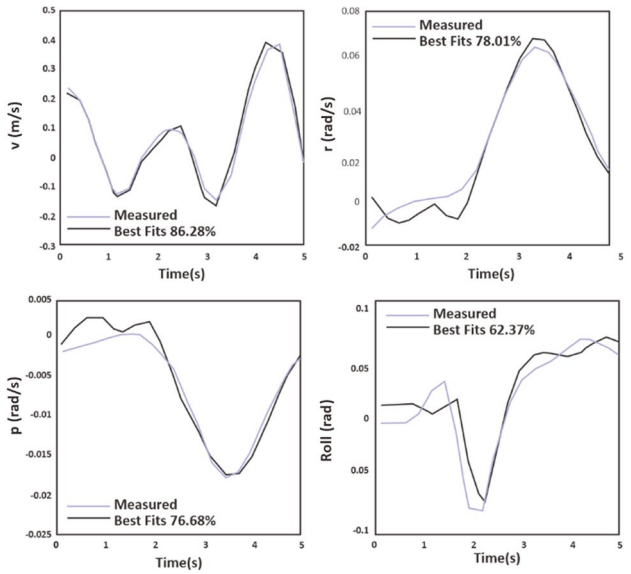

Fig. 17 Empirical model (lateral mode) validation results

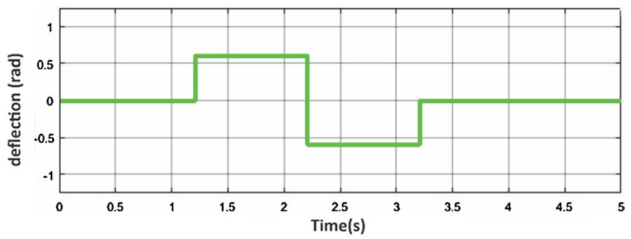

Fig. 18 Doublet input for all control surface, elevator (longitudinal mode) and aileron (lateral mode)

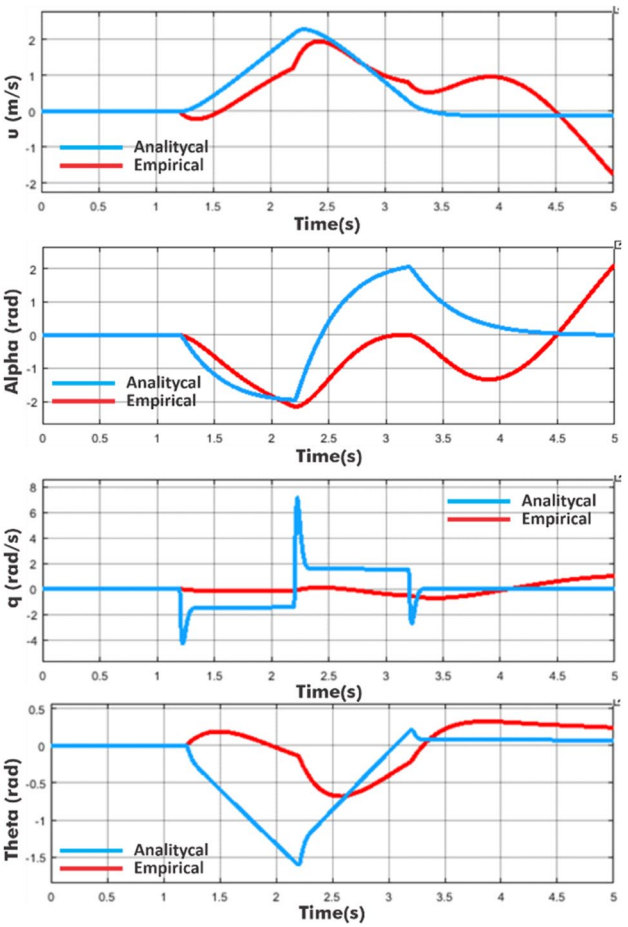

Fig. 19 Longitudinal mode comparative results: analytical models (blue) and empirical model (red) (Color figure online)

waveform. While the analytical model waveform goes up, the empirical model waveform also goes up or while one goes down, the other also goes down.

The modeling results or waveforms are influenced by many things. For example, if the empirical model waveform has a slight delay or lower amplitude than the analytical model, it can be caused by natural factors, such as wind. Due to the wind factor, the aircraft ordered by the operator/pilot to turn right for example, at the same time, there is a strong wind from the right side, then the response of the aircraft will be a bit late. Flight data acquisition was performed in the morning when the wind blows low enough and the weather is in a clear condition. However, these conditions can only be observed at the ground level, while conditions in the height were unknown. Flying scenarios can also affect the modeling results. The aircraft was flown manually, all scenarios were determined by feeling from the operator/pilot. The modeled aircraft has a small size with a flying wing configuration. This configuration needs high accuracy and responsive control. With a little change in the control surfaces, the aircraft's attitude and position change quickly.

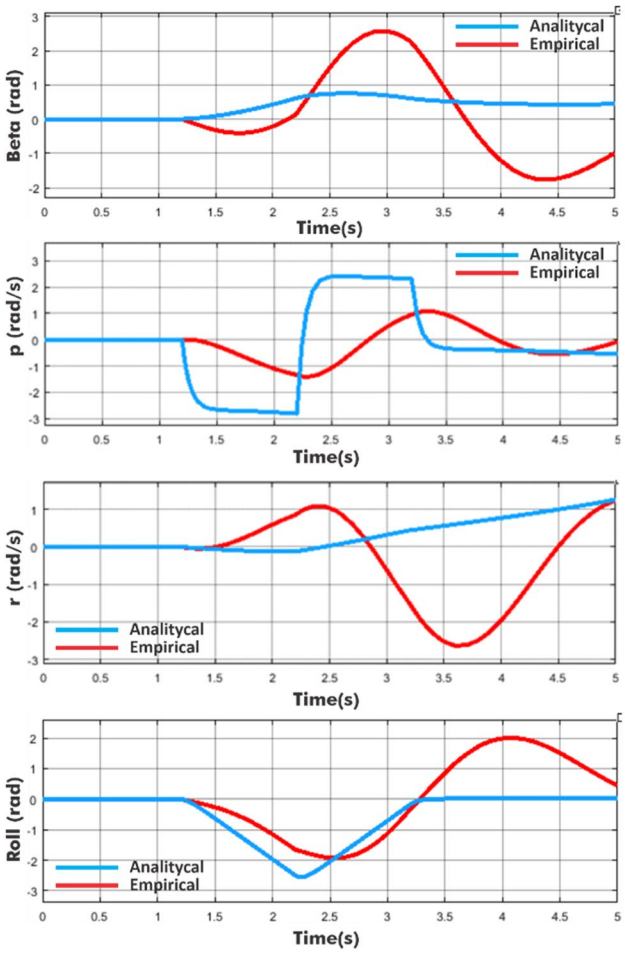

Fig. 20 Lateral mode comparative results: analytical models (blue) and empirical model (red) (Color figure online)

This happened in inflight data acquisition. The aircraft is quite difficult to be directed in trim conditions. Trim state parameters are important in aircraft modeling, as they were used as initial conditions, both for analytical and empirical modeling. The other difficulties also occur, when there is input variation in aileron input, the plane turns directly and at the same time loses altitude altogether. This causes the pilot to perform elevation recovery with elevators, so the expected scenarios are difficult to do.

From the analytical modeling can also be discussed some things that influenced the results. The UX-6 UAV is a small-size UAV with very low cruising speeds when compared with manned aircraft. Datcom + Pro software is designed for large aircraft with onboard pilots. Some research on UAVs modeling uses Datcom + Pro, but the average modeled aircraft is much larger than that used in this research. Datcom + Pro itself is less effective when used to calculate aircraft that has a low Reynolds number. Reynolds number is the ratio of inertial forces to viscosity (Ananda et al., 2016). With low cruising speeds, Datcom + Pro calculations will

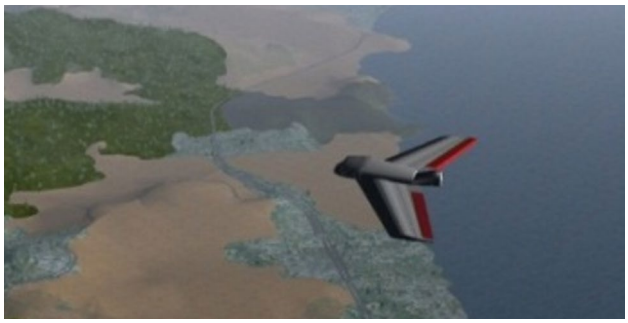

Fig. 21 UX-6 UAV simulation on Flight Gear flight simulator

be less precise. From Datcom + Pro results, UX-6 UAV has Reynolds number 1,020,300/m, this value is very small compared with the T-34 Charlie manned training aircraft, which has Reynolds number 4,813,500/m or Boeing 737–300 aircraft that has Reynolds number 60,363,000/m (Galbraith, 2015).

3.5 Visualization Result

The UX-6 UAV analytical model was visualized using Flight Gear flight simulator and MATLAB Simulink. Figure 21 is the result of visualization of UX-6 UAV.

4 Conclusions

This work shows that the analytical model can be used as a base for the development of UX-6 UAV autonomous control systems, evidenced by validation with the empirical model. The modeling implemented in this research is influenced by three aspects. First, the calculation of aerodynamic coefficients of Datcom + Pro software is less accurate when used for calculations of small unmanned aircraft (low Reynolds number). Second, natural factors such as wind and thermal. Third, the disturbance from actuator vibrations and the electromagnetic field of the electronic device of the aircraft that could affect the reading of the instrumentation on the aircraft. The results and methods used in this research can be considered to develop a flying model for small UAVs such as the UX-6 UAV.

Acknowledgements Thanks to Aerospace and Satellite Study Center Universitas Gadjah Mada (UGM), for technical supports. Thanks also to the Board of Publisher and Publication Universitas Gadjah Mada (UGM) for the scientific writing Grant (Number 765/BPP/2018).

References

Aarenstrup, R. (2015). *Managing model based design*. The MathWorks Inc.

Ananda, G. K., Sukumar, P. P., & dan Selig, M. S. (2016). Measured aerodynamic characteristics of wings at low Reynolds numbers. *Procedia Computer Science, 29*, 1193–1202.

Bagheri, S. (2014). "*Modeling, simulation and control system design for civil unmanned aerial vehicle (UAV)*, " M. Eng. Thesis, Umeå University, Umeå, Sweden.

Dhewa, O. A., Dharmawan, A., & Priyambodo, T. K. (2017). Model of linear quadratic regulator (LQR) control method in hovering state of quadcopter. *Journal of Telecommunication, Electronic, and Computer Engineering, 9*(3), 135–144.

Galbraith, B. (2015). *Datcom+Pro user's manual*. Holy Cow Inc.

Majid, A., Sumiharto, R., & Wibowo, S. B. (2015). Identifikasi model Dari Peswat Udara Tanpa Awak Sayap Tetap Jenis Bixler. *Indonesian Journal of Electronics Instrumentation System (IJEIS), 5*, 43–54.

Mathwork (2015). "*Fly The Havilland Beaver*,". [Online]. Available: https://www.mathworks.com/help/aeroblks/examples/fly-the-dehavilland-beaver.html.

Napolitano, A. D. (2012). *From Modeling to Simulation*. Wiley.

Nelson, R. C. (1998). *Flight stability and automatic control* (2nd ed.). McGraw-Hill Int.

Priyambodo, T. K., & Dharmawan, A. (2017). Auto Vertical Takeoff and Landing on Quadcopter using PID-fuzzy. *Journal of Engineering and Applied Sciences, 12*, 6420–6425.

Priyambodo, T. K., Dharmawan, A., Dhewa, O. A., & Putro, N. A. S. (2016a). Design of Flight Control System for Flying Wing UAV Based on Pitch and Roll Rotation. *International Journal of Engineering Research and Management (IJERM), 03*, 51–54.

Priyambodo, T. K., Dharmawan, A., Dhewa, O. A., Putro, N. A. S. (2016). "Optimizing control based on fine tune PID using ant colony logic for vertical moving control of UAV system," in *AIP Conference Proceeding*, vol. 1755.

Smith, M.S., Moes, T.R. (2003) "Real-time stability and control derivative extraction from F15 flight data". In *AIAA Atmospheric Flight Mechanics Conference*.

Stevens, B. L., & dan Lewis, F. L. (2003). *Aircraft Control and Simulation* (2nd ed.). Wiley.

Tischler, M. B. (2006). *Aircraft and rotorcraft system identification, engineering methods with flight test example*. American Institute of Aeronautics and Astronautics.

Triputra, F., Trilaksono, B., Sasongko, R., dan Dahsyat, M. (2016). "Longitudinal dynamic system modeling of a fixed-wing UAV towards autonomous flight control system development -a case study of BPPT Wulung UAV Platform," in *International conference on system engineering and technology*.